KSCE Journal of Civil Engineering

DOI 10.1007/s12205-019-0470-y

Tunnel Engineering

pISSN 1226-7988, eISSN 1976-3808
www.springer.com/12205

An Efficient Computational Model for Simulating Stress-dependent Flow in Three-dimensional Discrete Fracture Networks

Soheil Mohajerani*, Gang Wang, Duruo Huang***, S. M. E. Jalali****, S. R. Torabi*****, and Feng Jin******

Received March 29, 2018/Accepted September 29, 2018/Published Online January 2, 2019

Abstract

In-situ modelling of stress-dependent fluid flow in fractured rocks is important for various applications in rock engineering. However, precise determination of the hydraulic aperture of subsurface fractures, particularly at great depths, is often quite difficult. One of the most important parameters affecting the aperture is the stress field. Therefore, in this study, a new FEM model is proposed to study the effect of the in-situ stresses on the flow rate in fractured rocks with limited fracture lengths using a one-way hydro-mechanical coupling scheme and various non-linear joint constitutive models. The model is computationally efficient and of low-cost for various applications, and it provides results that are consistent with those from time-consuming two-way coupling methods. A series of sensitivity analyses have also been carried out to investigate key parameters in the model and to demonstrate how the fracture aperture and fluid flow change with variation of the in-situ stress field.

Keywords: *discrete fracture network, joint constitutive model, finite element method, fluid flow, sensitivity analysis, fractured rock*

1. Introduction

Simulating the effects of stress on the permeability and fluid flow through rock masses is important in various fields in rock engineering, such as stability analyses of rock slopes, modeling of rock foundations, underground excavations, hydrocarbon and geothermal reservoirs, and nuclear disposal in fractured rocks, study of transmission of environmental contaminations in fractured media (Rutqvist and Stephansson, 2003). If the permeability of the rock matrix is negligible compared to the fracture, the fluid flow can be assumed to flow along paths created by the connected fracture network. The total permeability of the rock mass is affected by the geometry of fracture system and the in-situ stress field (Zimmerman and Main, 2004; Mohajerani *et al.*, 2017).

The fracture system in a rock mass is complex, because its geometrical configuration is difficult to be determined given limited in-situ measurements. Three-dimensional data obtained from conventional seismic methods do not always have sufficient resolution, and the use of micro-seismic data is still subjected to considerable restrictions in interpretation and calibration Moreover, geometrical data mapped from the drilled cores and well-logging (one-dimensional) or the surface of the outcrops and trenches (two-dimensional) contain a lot of uncertainties in the input parameters. To analyze such uncertainties in modelling subsurface fractures, the Discrete Fracture Network method (DFN) can be used by assuming that the geometrical parameters of the fractures are statistically distributed (Priest, 2012; Lee *et al.* 1999; Lei *et al*., 2017; Jeong *et al.* 2004; Jin *et al.* 2003). To create a three-dimensional DFN configuration, it is necessary to determine a number of geometrical parameters such as density, orientation and length of the joint sets in the fracture network (Latham *et al.,* 2013). The influence of the model parameters can be assessed when a large number of realizations by DFN models are used to simulate the hydro-mechanical behavior of the rock mass (Mohajerani *et al.*, 2017).

The other important parameter is the fracture aperture which

*Research Student, Faculty of Mining, Petroleum and Geophysics Engineering, Shahrood University of Technology, Shahrood 8165865893, Iran (E-mail: soheilmohajerani@gmail.com)
**Associate Professor, Dept. of Civil and Environmental Engineering, Hong Kong University of Science and Technology, Clear Water Bay, Kowloon, Hong Kong (Corresponding Author, E-mail: gwang@ust.hk)
***Assistant Professor, Dept. of Hydraulic Engineering, Tsinghua University, Beijing 100084, China (Corresponding Author, E-mail: huangduruo@tsinghua.edu.cn)
****Associate Professor, Faculty of Mining, Petroleum and Geophysics Engineering, Shahrood University of Technology, Shahrood 3619995161, Iran (E-mail: jalalisme@gmail.com)
*****Professor, Faculty of Mining, Petroleum and Geophysics Engineering, Shahrood University of Technology, Shahrood 3619995161, Iran (E-mail: rtorabi@shahroodut.ac.ir)
******Professor, Dept. of Hydraulic Engineering, Tsinghua University, Beijing 100084, China (E-mail: jinfeng@tsinghua.edu.cn)

cannot be precisely determined because of alteration and stress relaxation during excavations or tectonic processes such as folding, faulting and erosion (Bisdom *et al.*, 2016; Zareifard *et al.*, 2016; Son and Moon, 2017). At great depths, the permeability of rock mass is a function of the hydraulic fracture aperture, which is governed by the in-situ stress field and pore pressure of the fluid inside the fractures (i.e., effective stress) (Bisdom *et al.*, 2017; Gan and Elsworth, 2016, Farhadian *et al*., 2017). Therefore, in order to study the influence of the effective in-situ stress field on the permeability of fractured rocks, a Joint Constitutive Model (JCM) that controls the non-linear behavior of the hydraulic aperture against the effective stress field should be considered (Bandis, 1980; Xie *et al.*, 2014). In rock engineering and geoscience, the term "hydro-mechanical coupling" refers to the interaction between hydraulic and mechanical processes (Rutqvist and Stephansson, 2003). The influence of stresses on the fluid flow can be considered as a part of the hydro-mechanical coupling when stresses result in variations in hydraulic properties. The effects of the fluid flow on the stress field, and consequently deformation of the jointed rock mass, also need to be considered in a two-way hydro-mechanical coupling (Min *et al.*, 2004). To investigate the hydro-mechanical coupling, direct measurements using laboratory and in-situ tests with large-scale samples are technically possible. However, such experiments are very costly and the results cannot be generalized to other cases. Therefore, a large number of experimental, analytical and numerical methods have been developed to analyze the hydro-mechanical coupling. Despite of many analytical models, it is still challenging to determine the stress-dependent parameters in the model (Jing *et al.*, 2013; Mi *et al.*, 2016; Zhang *et al.*, 2007; Vairogs *et al.*, 1971).

In order to analyze the hydro-mechanical coupling in fractured rocks, the numerical models are divided into two main categories: discontinuum models and equivalent continuum models (Lei *et al.*, 2017). The former assumes that rock mass is an assimilation of discrete blocks separated by fracture planes. The fractures can be modeled either separately or as intersections of the discrete blocks. Small-scale behavior of the fracture network can be investigated by the latter method. However, its application in large-scale networks with a huge number of fractures is quite time-consuming and computationally expensive. Instead, the equivalent continuum models are prevalent due to use of simple continuum mechanical equations for the simulation of large-scale rock masses (Gan and Elsworth, 2016). One of the commonly used equivalent continuum models for hydro-mechanical coupling is the crack tensor theory developed by Oda (Oda, 1986), which has been used by many researchers (Gan and Elsworth, 2016; Ababou *et al.,* 2005; Hu *et al.,* 2013).

The Finite Element Method (FEM) is applicable for problems with a limited number of fractures (Beyabanaki *et al.*, 2009; Goodman *et al.*, 1968). The hydro-mechanical coupling for porous media has been simulated based on the Biot theory (Noorishad *et al.*, 1982; Xie and Wang, 2014; Ye and Wang, 2016; Ye *et al.*, 2016). A hybrid Boundary Element Method-Finite Element Method (BEM-FEM) was developed to compute the flow-displacement field in three-dimensional fractured models (Elsworth, 1986). Since then, a large number of discontinuum numerical methods have been studied for analyzing the hydro-mechanical coupling in fractured media using FEM (Minkoff *et al.*, 2003; Noorishad *et al.*, 1992; Rutqvist *et al.*, 1992), BEM (Jing *et al.*, 2001; Hyman *et al.*, 2014), Discrete Element Method (DEM) (Min *et al.*, 2013; Zhao *et al.*, 2013), Discontinuous Deformation Analysis (DDA) (Jing *et al.*, 2001; Hyman *et al.*, 2014) and hybrid methods (Lei *et al.*, 2017; Latham *et al.*, 2013). Due to the complexities in calculation of the stress-dependent flow rate in a three-dimensional fractured model, only a few studies have reported research on such topics.

In order to analyze the hydro-mechanical coupling in DFN frameworks using numerical methods, the geometrical domain of the model must be meshed using a robust discretization scheme. Various methods have been developed to handle the meshing challenges in a three dimensional DFN (Hyman *et al.*, 2014; Karimi-Fard and Durlofsky, 2016; Mustapha *et al.*, 2011; Erhel *et al.*, 2009; Berrone *et al.*, 2014; Mohajerani *et al.*, 2018). On the one hand, determination of the fluid flow at different depths below the ground surface is critical for various engineering applications, although the aperture characteristics of subsurface fractures as a key factor for computing the flow rate is difficult to assess.

Therefore, the main purpose of this research is developing a new computationally efficient and cost effective model to analyze the influence of in-situ stress fields on the flow rate in fractured rocks with limited fracture length. The solution scheme of the present model is structured based on FEM formulation of various non-linear Joint Constitutive Models (JCMs). Not only does this state-of-the-art scheme shrink the burden of the calculations of a hydro-mechanical coupling, but also it makes possible the modelling of limited persistent fractures. The solution of the model is achieved using the conjugate Gradient Method (CG), which is one of the most widely used iterative methods. The model is implemented in C# as a computer program named FlowSHUT^{3D} with a visual user interface displaying the results graphically and independent from the other programs. This program can receive the geometrical data directly from the field surveys, generate an arbitrary number of three-dimensional DFN realizations, triangulate the geometrical domain of the model using an optimized meshing algorithm (Erhel *et al.*, 2009) and predict the flow rate at different in-situ stress fields.

The following assumptions are considered in this research for simplification:

- The fractures are represented by a pair of parallel smooth planes with finite lengths.
- The rock matrix is impermeable and linearly elastic.
- The flow is in a steady state based on Darcy's law for a Newtonian fluid.
- The Representative Element Volume (REV) of the fractured media is a statistical representation of a much larger domain.

This paper is organized as follows: In Section 2, methodologies

for the generation of three-dimensional DFNs, refined conforming mesh technique, different JCMs, FEM and implementation of FlowSHUT^{3D} are described. In Section 3, the results of FlowSHUT^{3D} using several JCMs are firstly compared with the 3DEC program. Then, a series of sensitivity analyses on key parameters affecting the flow are provided.

2. Methodology

Full hydro-mechanical coupling involves complex interaction between mechanical and hydraulic processes (Jing *et al.*, 1995). However, from the hydraulic point of view, it is only possible to consider the stress-dependent flow rate as a one-way hydro-mechanical coupling. The one-way coupling can be validated as long as any change in the hydraulic condition would not significantly affect the geometry of DFN. Therefore, in this study, a new model is proposed to study the effect of the in-situ stresses on the flow rate using the one-way hydro-mechanical coupling and experimental JCMs. The model is computationally efficient and of low-cost for various applications.

2.1 Generation of DFN

DFN forms the geometrical framework of the developed model in this research. The process of generating DFN is described as follows. Based on the geological origin, rock fractures are grouped into joint sets with similar dip and dip direction. The joint sets are independently simulated and the final model is an assemblage of all of them. Any joint set is defined by geometrical distribution parameters such as the location, orientation (dip and dip direction) and the dimensions of the joint plane.

The center location of the fracture plane is the first parameter to be modeled. In this study, a homogenous Poisson process is used to determine coordinates of center points of fractures following Xu and Dowd (2010). First, the REV is subdivided into k subdomain. For each of the subdomain, the number of center points is evaluated as follows:

$$\mu_i = \lambda \cdot V_i \tag{1}$$

where V_i is the volume of the i^{th} subdomain, and λ is a constant fracture intensity in a three-dimensional space (the number of fracture planes per unit volume). Since the center of some of fracture planes may be located outside of the REV domain, their lengths can be large enough to enter the domain and affect the connectivity pattern of the network. Therefore, the generation domain of the fractures is considered to be several times larger than the REV domain at first, then, the cube of the REV domain is extracted from the larger domain after completing the generation process. For each of the subdomain, a random variable N_i, representing the number of fractures within the domain, follows the Poisson distribution as below:

$$P(N_i = n) = \frac{\mu_i^n}{n!} e^{-\mu_i} \tag{2}$$

After determining the number of fracture within a subdomain, coordinates of the center points can be determined within the subdomain following a uniform distribution. Fig. 1(a) illustrates the generated center locations of fractures.

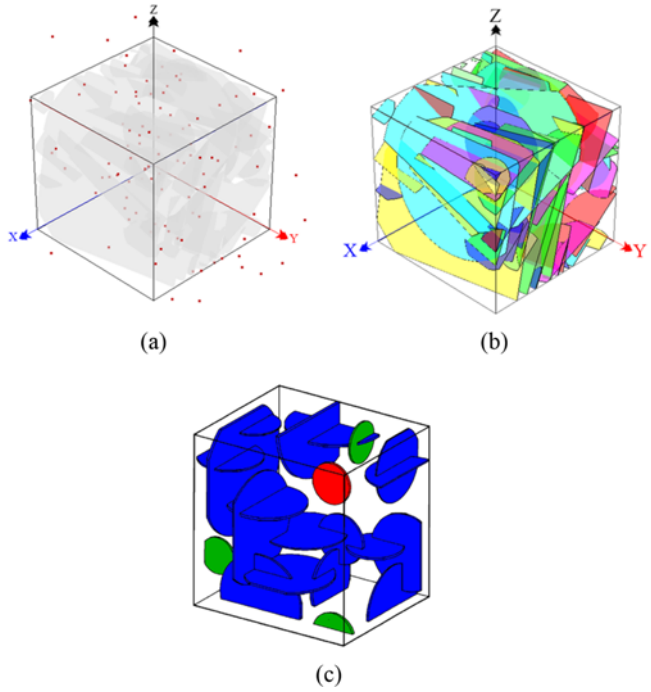

Fig. 1. Geometrical Framework of the Discrete Fracture Network: (a) the Center Location of Fractures, (b) a Realization of DFN Generated by FlowSHUT^{3D}, (c) a Schematic of Different Types of Fractures (Jing *et al.*, 2001): Single Fractures (red colored), Dead-end fractures (green colored) and Persistent Fractures (blue colored)

Following the location generation, the orientation and length of the fractures are generated using the Probability Distribution Functions (PDF) and the Monte-Carlo sampling technique. Usually, the uniform and Fisher PDFs are used to model the dip and dip direction respectively, and the rotation angle is modeled by the uniform PDF. The PDF of the fracture length (L) is usually a power-law or log-normal. The shape of the fractures is assumed to be circular, elliptical or polygonal. Then, the hydraulic parameters of the fractures, such as the aperture size and roughness, is assigned to the location of the fractures similar to the generation of geometrical parameters as required. The PDF of the aperture is usually uniform. In the literature, a number of equations have been suggested to determine the relation between the aperture and the length of fractures. An example of such an equation is given in Eq. (3) (Vermilye and Scholz, 1995) as follows:

$$a = \zeta\sqrt{L} \tag{3}$$

where a is the aperture size [mm], L is the length of fracture [m], and ζ is a constant coefficient determined by the condition of fractures (in a general case, $\zeta = 0.004$). As mentioned previously, after completing the process of fracture generation, the REV domain is extracted from the generation domain. Fig. 1(b) depicts a realization of DFN REV generated by FlowSHUT^{3D}.

Fractures can have one of the three main types of connectivity with the other fractures or boundaries of the model: the multiple connectivity (persistent fractures), only one connection (dead-end fractures) and no connection (single fractures). As shown in Fig. 1(c), the persistent fractures (blue colored) usually have longer lengths and several (at least two) intersections with the other fractures and/or boundaries. Such fractures can be intersected by the boundaries of the model or be connected to dead-end fractures and be completely located inside the model. Although dead-end (green colored) and single (red colored) fractures can have important effects on the ultimate strength and mechanical properties of the rock mass, they do not have a significant effect on the hydraulic properties (Jing, 2003). Since hydraulic analysis is the main aim of this research, it is reasonable to remove the dead-end and single fractures from the REV domain to improve the performance of the model, particularly when the model contains a great number of fractures.

2.2 Meshing Technique

There are serious challenges to discretize a three-dimensional DFN model into a high quality meshing structure. The elements of unstructured triangulation do not follow a uniform pattern. On the one hand, structured meshing is not convenient in representing the complex three-dimensional geometry of the fractured media. Specifically, a high quality unstructured meshing must be able to meet particular geometrical requirements (Mustapha *et al.,* 2011; Monteagudo and Firoozabadi, 2003). As shown in Fig. 1(b), a network of fractures generated statistically can include the fracture length varying over several orders of magnitude. Due to the complex structure of a three-dimensional DFN with arbitrary shape and spatial fracture position, it is possible to form intersection segments of fracture planes which are parallel or crossover on a third fracture plane. If the distance between two parallel intersections or the angle between two crossover intersections is too acute, low-quality meshing elements might be generated. These elements can result in an ill-conditioned discretizing matrix and cause numerical divergence (Hyman *et al.,* 2014).

In this study, the algorithm proposed by (Erhel *et al.*, 2009) is utilized to discretize DFN and address the aforementioned meshing challenges regarding complex three-dimensional geometries. This algorithm provides a triangulation that does not change the geometrical structure of DFN and consequently the connectivity pattern of the fractures (Mohajerani *et al.*, 2018). The triangulation of a single fracture with two orthogonal joint planes and a realization of DFN generated by FlowSHUT^{3D} are shown in Fig. 2.

2.3 Description of JCMs

Here, "aperture" refers to the normal distance between two fracture planes, and "closure" is the aperture variation due to the effect of normal stress. Eq. (4) is an experimental JCM that is especially applicable to DFN models, as suggested by Öhman (2005) as follows:

$$\textbf{JCM1: } a = \frac{a_f}{(1+\sigma_{en})^{\frac{2}{3}}} \tag{4}$$

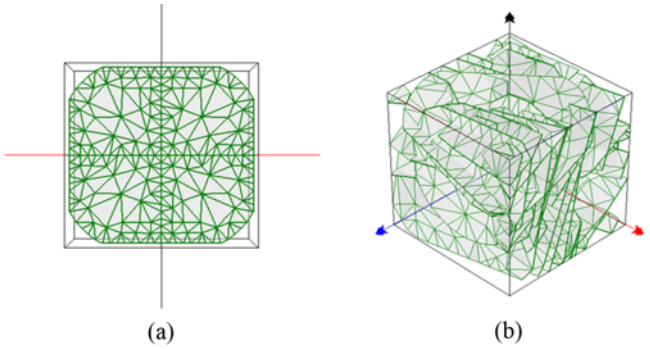

Fig. 2. Triangulation of: (a) a Single Fracture with Two Orthogonal Intersections, (b) a Realization of Three-dimensional DFN, Generated by FlowSHUT^{3D}, using Meshing Algorithm Provided in (Erhel *et al.*, 2009)

$$\sigma_{en} = \sigma_n - p_p \tag{5}$$

where a_f is the initial aperture of a fracture [mm], which is determined by in-situ or laboratory hydraulic tests, and σ_{en}, σ_n and p_p are the effective normal stress, total normal stress and pore pressure on a fracture plane respectively [MPa]. The equation shows how the joint aperture (a) reduces with increasing effective normal stress. An alternative experimental JCM has been provided by Raghavan and Chin (2002) as follows:

$$\text{JCM2: } a = a_f e^{-0.5(\rho\sigma_{en})} \tag{6}$$

where ρ is a constant empirical coefficient such that $6.895 \times 10^{-7} \le \rho \le 6.895 \times 10^{-6}$.

One of the commonly used constitutive models to simulate the non-linear closure of fractures subjected to normal effective stress is introduced by Bandis *et al.* (1983) as follows:

$$\text{JCM3: } \delta = \frac{\sigma_{en}\delta_m}{k_{n0}\delta_m + \sigma_{em}} \tag{7}$$

where, δ and δ_m are closure and maximum closure of the fracture [mm], and k_{n0} is the normal fracture stiffness [MPa/mm]. k_{n0} and δ_m are calculated from Eqs. (8) and (9) respectively as follows (Bandis *et al.*, 1983):

$$k_{n0} = -7.15 + 1.75JRC + 0.02 \times \frac{JCS}{a_f} \tag{8}$$

$$\delta_m = -0.1032 - 0.0074JRC + 1.1350 \times \left(\frac{JCS}{a_f}\right)^{-0.2510} \tag{9}$$

where JCS is the joint compressive strength [MPa] and JRC is the joint roughness coefficient. It should be noted that JRC and JCS are scale-dependent and should be modified according to the desired scale.

In the end, the fracture aperture (a) is determined from Eq. (10) as follows:

$$a = a_f - \delta \tag{10}$$

The permeability is calculated based on the Poiseuille law (Eq. (11)) with the assumption of the fracture with unit width as

follows:

$$\bar{k}_f = \frac{a^3}{12} \tag{11}$$

Note that $\bar{k}_f$ is only for the mean fracture behavior. By assuming the permeability is log-normally distributed, Eq. (12) can be used to statistically represent the permeability of an arbitrary fracture (Öhman *et al.*, 2005) as follows:

$$k_f = 10^{Log(\bar{k}_f) + Log(t)} \tag{12}$$

where t is a variable of the normal PDF representing the intrinsic variability of the permeability. In this research, Eqs. (13) and (14) have been used to simulate the in-situ stress field (Hoek *et al.*, 2000) as follows:

$$\sigma_V = \rho_r g h \tag{13}$$

$$\sigma_H = k\sigma_v \tag{14}$$

where σ_V and σ_H are the vertical and horizontal components of the in-situ stress field [MPa], ρ_r is the density of the rock matrix [kg/m^3], h is depth of the location of fracture from the ground surface [m] and k is the horizontal to vertical ratio of the stress field. The normal component of the in-situ stress field on each fracture plane (σ_n) is obtained using stress transformation.

2.4 The Solution Scheme

The planar flow rate is calculated on each fracture of the network with an initial aperture of a_f. It is assumed that $a_f \ll L_f$, where L_f is the length of the fracture. In this research, a uniformly distributed PDF has been used to determine a_f. The permeability of the fracture (k_f) is obtained using Eq. (11) according to the Poiseuille law (Baca *et al.*, 1984).

The fracture aperture a is determined based on the JCMs described in Section 2-3. As given in Eq. (15), Darcy's law and mass conservation govern the fluid flow through fractured rock media (Koudina *et al.*, 1998) as follows:

$$\begin{cases} v = -\dfrac{1}{\mu} k_f \cdot \nabla p \\ \nabla v = 0 \end{cases} \tag{15}$$

where μ is dynamic viscosity [Pa·s], v is the locally averaged flux (flow rate per unit area) [m/s], k_f is the intrinsic permeability of the fracture [m^2], ∇p is pressure gradient [Pa/m], $\nabla p = \rho g \nabla h$, where ρ is the fluid density [kg/m^3], g is the gravitational acceleration [m/s^2] and ∇h is hydraulic head gradient.

The Dirichlet and Neumann boundary condition can be applied to this system on the parts of REV denoted as Γ_D and Γ_N respectively as follows:

$$\begin{cases} h = h_D \quad on \quad \Gamma_D \\ v \cdot n = v_N \cdot n \quad on \quad \Gamma_N \end{cases} \tag{16}$$

where h_D and v_n are the prescribed hydraulic head and flux on the Dirichlet and Neumann boundary. As given in Eqs. (17), the total permeabilty matrix (K), the total vector of volumetric flow rate (q) and hydraulic head (h) for a DFN model are derived by assembling local quantities respectively as follows:

$$K = \begin{bmatrix} K_{11} & K_{12} & \cdots & K_{1\dot{N}} \\ K_{21} & K_{22} & \cdots & \vdots \\ \vdots & \vdots & \ddots & \vdots \\ K_{\dot{N}1} & \cdots & \cdots & K_{\dot{N}\dot{N}} \end{bmatrix}, \; q = \begin{pmatrix} q_1 \\ \vdots \\ \vdots \\ q_{\dot{N}} \end{pmatrix}, \; h = \begin{pmatrix} h_1 \\ \vdots \\ \vdots \\ h_{\dot{N}} \end{pmatrix} \tag{17}$$

where, $\dot{N} = N_{v_i} \times N_{dof_i}$, and N_{v_i} and N_{dof_i} are the total number of vertices and the degrees of freedom of the model respectively. The hydraulic head must be determined in all vertices of the model. In this research, this system of equations is solved using a FEM scheme. The Conjugate Gradient method (CG) is used to calculate the final results of the system.

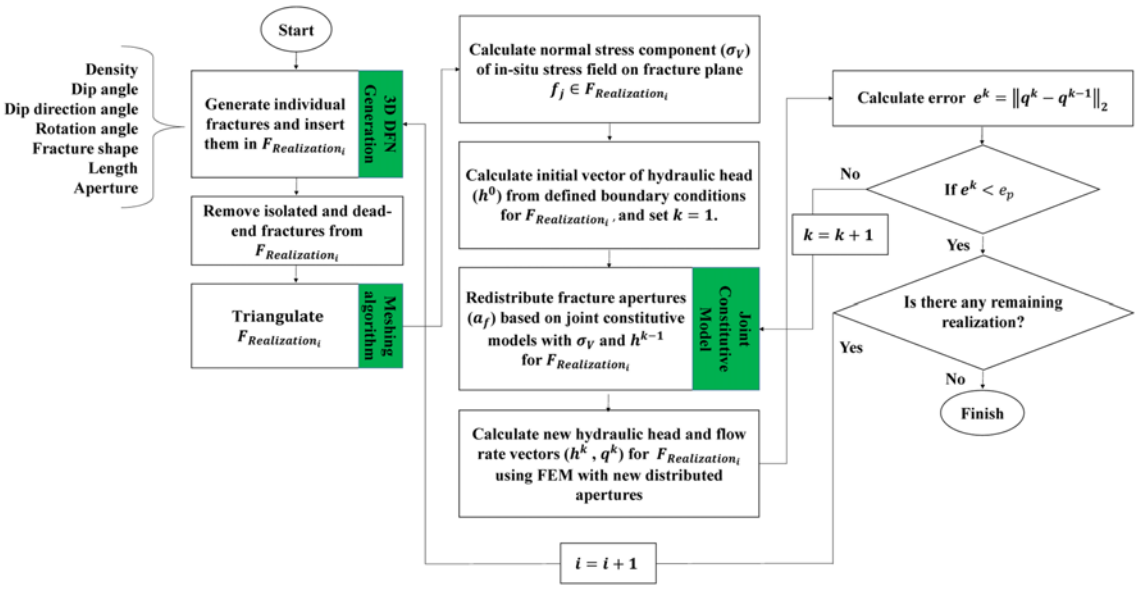

Fig. 3. Flowchart of the Algorithm to Analyze the Stress-dependent Flow Field

2.5 Algorithm Implementation

In this section, the algorithm to analyze the stress-dependent flow rate in FlowSHUT^{3D} is illustrated. The developed algorithm is implemented in C# with a graphical user interface to visualize the results. According to the flowchart depicted in Fig. 3, the algorithm includes the following steps:

1 DFN is created based on input geometrical - statistical data and the method described in Section 2-1. In order to evaluate the variation in calculations, thirty independent realizations of the same DFN are generated. The total flow field of the model is averaged based on all realizations.
2. For each realization, the isolated and dead-end fractures are removed from the domain.
3. The modified realization (obtained from step 2), is triangulated using the algorithm introduced in Section 2-2.
4. Using the total in-situ stress field calculated for the center of the model, σ_n is determined on each fracture plane with the aid of tensor transformation.
5. In the initial step of the iteration ($i = 1$), the hydraulic head vector (h^0) is considered zero for non-boundary vertices and initialized for boundary vertices. For steps $i \geq 2$, this vector equates the hydraulic head calculated in the step $i-1$, (h^{i-1}).
6. The aperture is redistributed using the JCM (Section 2-3) by computing the normal effective stress ($\sigma_{en}^i = \sigma_n - (\rho_f g h^{i-1})$) for each element of the triangulation, whereby, the corresponding k_f^i is calculated.
7. The vector h^i is calculated using the scheme described in Section 2-4 and the FEM formulation. Then, the flow rate vector is calculated as $q^i = [K]h^i$.
8. The error $|e^i| = \|q^i - q^{i-1}\|_2 / \|q^i\|_2 \times 100\%$ is calculated where $\|\cdot\|_2$ is Euclidean norm. If $|e^i|$ is smaller than the desired precision of the problem (e_p), the algorithm goes to the step 9, otherwise, steps 5 to 8 are repeated.
9. The iteration loop is completed and q^i is introduced as the ultimate vector of the stress-dependent flow rate for each realization.
10. The algorithm goes to the step 2 to solve the problem for the next realization. If there is no any other realization, the algorithm is terminated.

3. Results and Discussion

In this section, the stress-dependent flow rate is analyzed by FlowSHUT^{3D} using different JCMs, and the results are also compared with other two-way coupling models for model validation. Numerical convergence and sensitivity analysis of key parameters are also discussed.

3.1 Model Validation

In order to validate the present model, the calculated results of FlowSHUT^{3D} are compared with 3DEC using three different JCMs described in Section 2-3. 3DEC is a three-dimensional commercial program based on DEM for discontinuum modeling of hydro-mechanical couplings. Practically, 3DEC modelling is a two-way coupling method. In the first step (mechanical step), 3DEC balances the model with fluid pressure and in-situ stress, and adjusts the equivalent fractures aperture. In the second step (hydraulic step), it calculates the hydraulic field in the model based on the equivalent aperture. 3DEC is able to simulate the response of a discontinuum medium (e.g., fractured rock) exposed to static loading. Therefore, such modelling is considered as an assimilation of discrete blocks and discontinuities forming the boundaries of these blocks (Itasca, 2004). To model the hydro-mechanical coupling processes in 3DEC, it is necessary to discretize each block independently so as to apply Finite Difference Method (FDM). In this way, a hybrid FDM-DEM scheme is implemented to solve the stress-dependent flow problem.

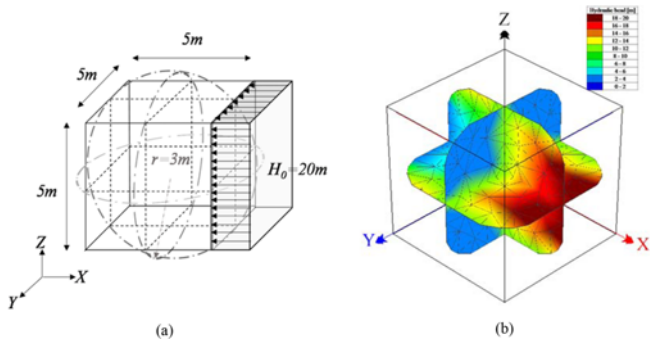

Fig. 4. Input Geometrical Parameters, Boundary Conditions and Results of Flow SHUT^{3D} Calculations: (a) the Geometrical Structure and Boundary Conditions, (b) the Diagram of Hydraulic Head Distribution calculated by FlowSHUT^{3D}

The geometrical structure and boundary conditions of the model are shown in Fig. 4(a). The model domain is a cube with dimensions of 5 × 5 × 5 m with the geometrical center located at the origin of the coordinates. Three orthogonal circular fractures with radius of 3 m, the center located at the origin of the coordinates and an aperture of 1 mm, are embedded in the model. A constant hydraulic head of 20 m has been applied on the right facet of the model with the other boundary conditions considered zero. The geomechanical and rheological parameters of the model are listed in Table 1. For comparison, the vertical in-situ stress changes from 10^{-1} to 10^{1} MPa in several levels and the flow rate on the left boundary of the model is calculated subsequently. The diagrams of hydraulic head distribution of the model calculated by FlowSHUT^{3D} are shown in Figs. 4(b). Note that 3DEC doesn't consider JCS and JRC directly, but it requires estimation of the normal stiffness (k_n) of the joints using JCS and

Table 1. Geomechanical and Rheological Parameters of the Model

Parameter	Value	Parameter	Value
ρ_r [kg/m^3]	2,500	a_f [m]	0.001
k_n [GPa/m]	1.32	ρ_f [kg/m^3]	1,000
JCS [MPa]	50	μ [Pa.s]	0.001
JRC	5	g [m/s^2]	9.81
K [GPa]	1		
G [GPa]	1		

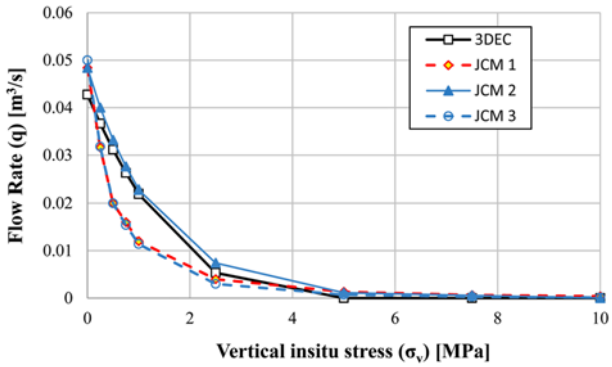

Fig. 5. Volumetric Flow Rate (q) Versus Vertical In-situ Stress (σ_v) calculated by FlowSHUT^{3D} using Three Different JCMs (Eqs. (4)-(6)) and 3DEC. The Flow Rate Exponentially Decreases with Increasing Vertical In-situ Stress with a Similar Trend for All the Models

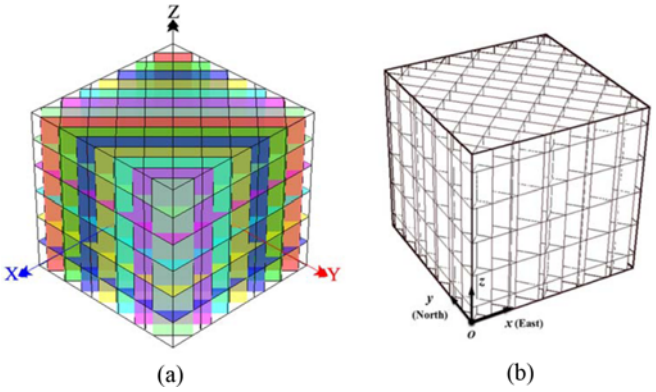

Fig. 6. Geometrical Structure of the Fracture Network Consisting of Three Orthogonal Sets of Persistent Fractures Generated by: (a) FlowSHUT^{3D}, (b) Lei *et al.* (2015)

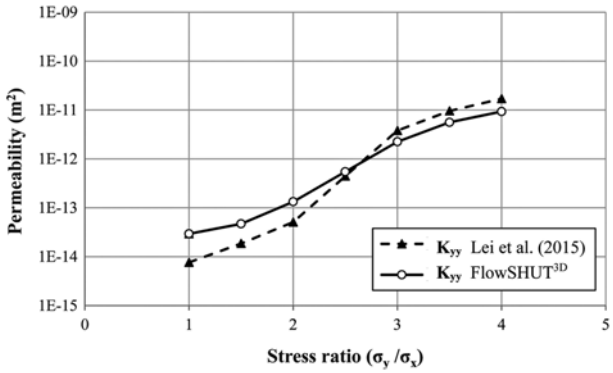

Fig. 7. Permeability (K_{yy}) versus Stress Ratio (σ_y/σ_x) Calculated using FlowSHUT^{3D} and Lei *et al.* (2015)

JRC.

Volumetric flow rate passing through the model domain boundary is shown in Fig. 5. It is observed that the flow rate exponentially decreases with increasing vertical in-situ stress. The decreasing trend is similar for all simulations using constitutive models JCM1, JCM2, JCM3 and 3DEC, while the start and end points of the results are almost the same. The biggest difference appears in range of applied stress smaller than 3MPa. It is noted that JCM1 and JCM2 are developed for a network of fractures with many and a few of fractures respectively, while JCM3 has been widely used by a number of researchers for a single fracture. JCM1 is said to provide more realistic results in low stress level according to Öhman *et al.* (2005). For the simple fracture network tested in this study, it seems that both JCM1 and JCM3 yield similar results.

In this study, FlowSHUT^{3D} is also compared with a two-way coupling model developed by Lei *et al.* (2015) for model validation. The simulation domain is a 0.5 × 0.5 × 0.5 m^3 cube which consists of three orthogonal sets of persistent fractures. The geometrical parameters are summarized in Table 2. Figs. 6(a) and 6(b) show geometrical structure of the model in FlowSHUT3D and in Lei's research, respectively. The rock density, JCS and JRC are 2,700 Kg/m^3, 120 MPa and 15 respectively. The model is subjected to a deviatoric stress, where the vertical in-situ stress is 10 MPa, the horizontal component of the in-situ stress in X-direction is 5 MPa. The ratio of Y- versus X-component of the horizontal in-situ stress changes from 1 to 4. The JCM3 model (Bandis *et al.*, 1983) is used in the simulation to take account the effect of JCS and JRC. The equivalent permeability K_{yy} of the model is shown in Fig. 7. Despite of different physical conditions employed in two models, their results have similar increasing trend and generally agree very well with each other.

Table 2. Geometrical Parameters of the Fracture Network Containing Three Orthogonal Sets of Persistent Fractures

Fracture set	Dip [Deg]	Dip direction [Deg]	Spacing [m]	Aperture [mm]
Set 1	90	45	0.05	0.3
Set 2	90	315	0.075	0.3
Set 3	0	0	0.1	0.3

The above case studies validated the proposed one-way coupling method. The use of experimental JCM makes the algorithm fast and cost effective as compared with complicated two-way coupling methods.

3.2 Sensitivity Analyses

In this section, JM1 selected for sensitivity analyses to study the influence of joint geometry and in-situ stress on the flow. Four joint sets are simulated in a DFN model with dimensions of 5 × 5 × 5 m^3 with the geometrical center located at the origin of the coordinate system. The geometrical-statistical parameters functioned to generate the network are given in Table 3. Thirty independent REV realizations are generated to assess the variability of the results. The geomechanical and rheological properties of the model are given in Table 1. A hydraulic head of 20 m is applied on its right facet of the model and the other boundary heads are set to zero. A diagram of the hydraulic head distribution of the model for one of the realizations is shown in Fig. 8.

In this study, the computational error $\bar{e}$ is defined as:

Table 3. Geometrical – Statistical Parameters of the Joint-sets

Parameter	Dip [Deg]	Dip direction [Deg]		Density [1/m^3]	Length [m]			Aperture [mm]	
Joint-set	Uniform	Fisher		Poisson	Power-law			Uniform	
	Average	k	Average	Average	α	Min	Max	Min	Max
1	70	40	45	0.2	1.78	1	10	4	12
2	30	20	135	0.12	1.78	1	10	4	12
3	80	40	135	0.1	1.78	1	10	4	12
4	45	20	315	0.15	1.78	1	10	4	12

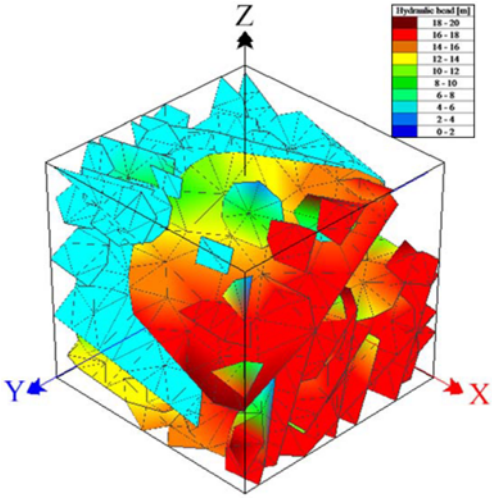

Fig. 8. Hydraulic Head Distribution for a Random Realization calculated by FlowSHUT^{3D}

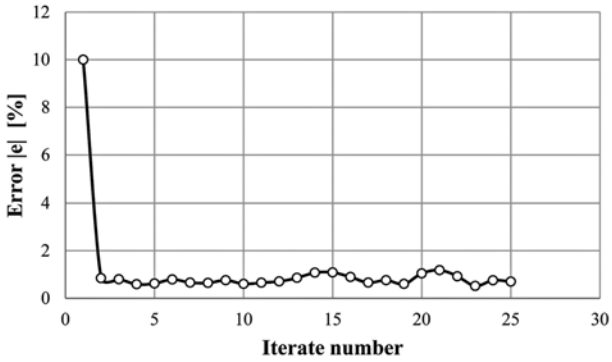

Fig. 9. The Computational Error |e| versus the Number of Iterations of the Model. |e| Converges Approximately to 0.7%

$$\bar{e} = |e^i| = \frac{\|q^{i-1} - q^i\|_2}{\|q^i\|_2} \times 100\% \quad (18)$$

where q^{i-1} and q^i are the flow rate vectors in the previous and current iterations respectively.

Figure 9 shows that the computational error ($\bar{e}$) diminishes quickly with increasing number of iterations, and $\bar{e}$ converges to an average value of 0.7% just within a few iterations. However, the number of iterations and the convergence value may be different for other realizations. This figure demonstrated that the convergence of the present algorithm is fast, therefore, all the following sensitivity analyses have been done using only five iterations to ensure convergence of the solution. For all tests conducted in this study, all results reach convergence. Therefore, this algorithm guarantees the convergence of the solution to a large extent with appropriate accuracy for the problem.

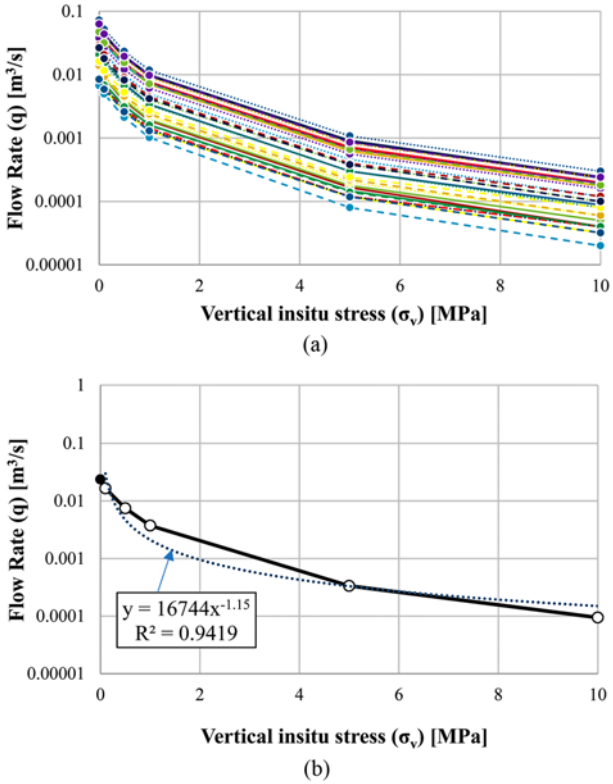

Fig. 10. The Chart of Vertical In-situ Stress versus: (a) the Flow Rate for Different Realizations, (b) the Median Flow Rate of the Model in Log Space (The fitting line is in dash.)

Since prediction of fluid behavior in rock masses under a predominant in-situ stress field is important in rock engineering applications, the effect of stress field on the fluid flow is considered in the following parametric study. To assess the variability of the model, a large number of DFN simulations are performed. The effect of σ_V on the flow rate for thirty different realizations of DFN has been compared in Fig. 10(a). The horizontal to vertical in-situ stress ratio is assumed as $k = 1$ in this analysis ($\sigma_V = \sigma_x = \sigma_y$). All the realizations show the same decreasing trend, however, the flow rates in the various stress levels may be very different for different realizations. This variability in a DFN model is due

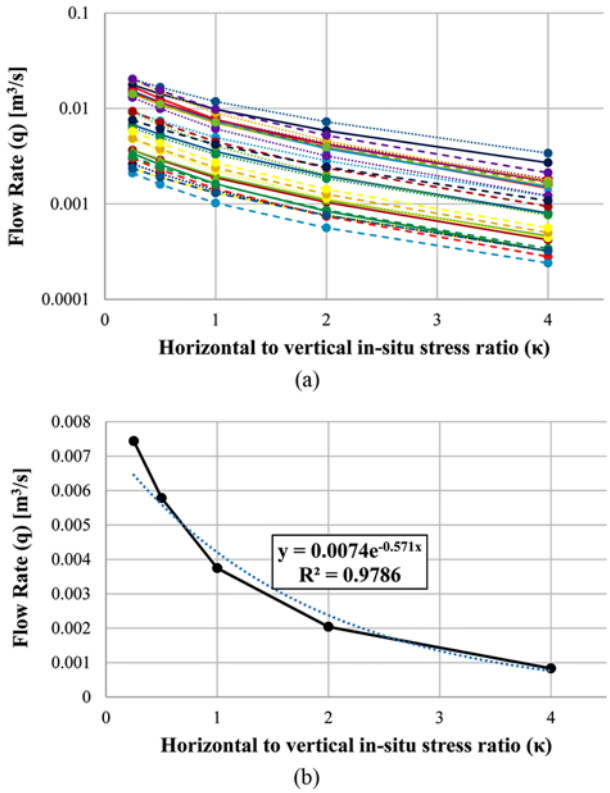

Fig. 11. The Flow Rate versus Horizontal to Vertical In-situ Stress Ratio for two Different Configuration of Calculations: (a) Flow Rate versus Horizontal to Vertical In-situ Stress Ratio (κ) for 30 Realizations, (b) Median Flow Rate in Natural Log Space versus Horizontal to Vertical In-situ Stress Ratio (κ)

to the stochastic nature of the joint distribution, which is modeled through multiple realizations.

In order to quantify the total flow rate for REV of DFN, in Fig. 10(b), σ_V versus the median flow rate of the model is fitted using the following equation with a coefficient of determination $R^2 = 0.94$:

$$q(m^3/s) = 16744\,\sigma_V^{-1.154}(Pa) \tag{19}$$

The flow rate is approximately uniformly distributed in natural-log space, and its standard deviation (in log space) can be quantified as follows:

$$\sigma_{lnq} = 0.757 \tag{20}$$

Note that the standard deviation is evaluated in natural logarithmic space. In other words, the value for one standard deviation above the median is about 2 times of the median value, the value for one standard deviation below the median is about 1/2 of the median value.

To study the influence of the deviatoric stress, simulations are conducted by assuming a fixed vertical stress $\sigma_V = 1$ MPa, and $\sigma_x = \sigma_y = k\,\sigma_V$, where k is the ratio of horizontal to vertical in-situ stress. The flow rate is represented in Fig. 11 for a varying k for 30 random realizations of DFNs. As in Fig. 11(a), with an increasing k, the flow rate decreases exponentaially for all realizations. An empirical equation has been derived by fitting the median flow rate using Eq. (21) with a coefficient of determination $R^2 = 0.98$ as follows:

$$q(m^2/s) = 0.0074e^{-0.571k} \tag{21}$$

Again, the flow rate is found to be uniformly distributed in the natural-log space with a standard deviation of $\sigma_{lnq} = 0.757$.

4. Conclusions

In this research, the dependence of flow rate on the in-situ stress has been investigated using a three-dimensional discrete fracture network. A new model has been developed and its corresponding program FlowSHUT^{3D} has been implemented, which is computationally efficient and of low-cost. The model efficiency lies in the fact that time-consuming two-way hydro-mechanical coupling are substituted by a one-way coupling scheme using an experimental JCM. Not only have the results in calibration section proven that the current model agrees well with other models using a two-way hydro-mechanical coupling, but also it converges to the solution in a few iterations.

The process of generating a three-dimensional discrete fracture network has been illustrated with describing an optimized conforming meshing algorithm. FlowSHUT^{3D} has been validated for three joint constitutive models in comparison to the well-known commercial program 3DEC. Besides, regarding the convergence of the model, a series of sensitivity analyses has been conducted on the both the vertical component and the horizontal to vertical ratio of the in-situ stress field for different realizations of DFN. In addition, the effects of the vertical in-situ stress on the fracture aperture, the number of iterations of the model on convergence of the solution and the amount of computational error are discussed. The results show that as the vertical component and the horizontal to vertical ratio of the in-situ stress field increases, the flow rate of the model decreases. Variability of the simulations is mainly due to the stochastic nature of the fractures properties, which can be quantified through a large number of simulations using random DFN realizations.

Yet, it should be also noted that the one-way coupling scheme assumes that mechanical deformation of the joint system is only represented by change in fracture aperture, and would not significantly change connectivity of the facture network. Limitation of the current model should be carefully evaluated for future use.

Acknowledgements

The authors acknowledges support from Joint Research Fund for Overseas Chinese Scholars and Scholars in Hong Kong and Macao (Grant No. 51828902) from National Natural Science Foundation of China and Theme-based Research Scheme Grant No. T22-603-15N from the Hong Kong Research Grants Council.

References

Ababou, R., Canamoni, I., and Elorza, F. J. (2005). “Thermo-hydro-

mechanical simulation of a 3D fractured porous rock: Preliminary study of coupled matrix-fracture hydraulics." *Proc. the Comsol Multiphysics Conference,* France, pp. 193-198.

Baca, R., Arnett, R., and Langford, D. (1984). "Modelling fluid flow in fractured porous rock masses by finite element techniques." *International Journal for Numerical Methods in Fluids*, Vol. 4, No. 4, pp. 337-348, DOI: 10.1002/fld.1650040404.

Bandis, S. (1980). *Experimental studies of scale effects on shear strength, and deformation of rock joints*, PhD Thesis, University of Leeds, Leeds, UK.

Bandis, S., Lumsden, A., and Barton, N. (1983). "Fundamentals of rock joint deformation." *International Journal of Rock Mechanics and Mining Sciences*, Vol. 20, pp. 249-268, DOI: 10.1016/0148-9062(83)90595-8.

Berrone, S., Fidelibus, C., Pieraccini, S., and Scialo, S. (2014). "Simulation of the steady-state flow in discrete fracture networks with non-conforming meshes and extended finite elements." *Rock Mechanics and Rock Engineering*, Vol. 47, No. 6, pp. 2171-2182, DOI: 10.1007/s00603-013-0513-5.

Beyabanaki, S. A. R., Jafari, A., Biabanaki, S. O. R., and Yeung, M. R. (2009). "A coupling model of 3-D discontinuous deformation analysis (3-D DDA) and finite element method." *Arabian Journal for Science and Engineering*, Vol. 34, No. 2B, pp. 107-119.

Bisdom, K., Bertotti, G., and Nick, H. M. (2016). "A geometrically based method for predicting stress-induced fracture aperture and flow in discrete fracture networks." *AAPG Bulletin*, Vol. 100, No. 7, pp. 1075-1097, DOI: 10.1306/02111615127.

Bisdom, K., Nick, H., and Bertotti, G. (2017). "An integrated workflow for stress and flow modelling using outcrop-derived discrete fracture networks." *Computers & Geosciences*, Vol. 103, pp. 21-35, DOI: 10.1016/j.cageo.2017.02.019.

Carpenter, C. and Practical, A. (2015). "Simulation method capturing complex hydraulic-fracturing physics." *Journal of Petroleum Technology*, Vol. 67, No. 10, pp. 81-83.

Elsworth, D. (1986). "A hybrid boundary element-finite element analysis procedure for fluid flow simulation in fractured rock masses." *International Journal for Numerical and Analytical Methods in Geomechanics,* Vol. 10, No. 6, pp. 569-584, DOI: 10.1002/nag.1610100603.

Erhel, J., De Dreuzy, J-R., and Poirriez, B. (2009). "Flow simulation in three-dimensional discrete fracture networks." *SIAM Journal on Scientific Computing*, Vol 31, No. 4, pp. 2688-2705, DOI: 10.1137/080729244

Farhadian, H., Hassani, A., and Katibeh, H. (2017). "Groundwater inflow assessment to Karaj Water Conveyance tunnel, northern Iran." *KSCE Journal of Civil Engineernig*, Vol. 21, No. 6, pp. 2429-2438, DOI: 10.1007/s12205-016-0995-2.

Gan, Q. and Elsworth, D. (2016). "A continuum model for coupled stress and fluid flow in discrete fracture networks." *Geomechanics and Geophysics for Geo-Energy and Geo-Resources*, Vol. 2, No. 1, pp. 43-61, DOI: 10.1007/s40948-015-0020-0.

Goodman, R. E., Taylor, R. L., and Brekke, T. L. (1968). "A model for the mechanics of jointed rocks." *Journal of Soil Mechanics & Foundations Division,* Vol. 94, No. 3, pp. 637-660.

Hoek, E., Kaiser, P. K., and Bawden, W. F. (2000). *Support of underground excavations in hard rock*, CRC Press.

Hu, L., Winterfeld, P. H., Fakcharoenphol, P., and Wu, Y.-S. (2013). "A novel fully-coupled flow and geomechanics model in enhanced geothermal reservoirs." *Journal of Petroleum Science and Engineering*, Vol. 107, pp. 1-11, DOI: 10.1016/j.petrol.2013.04.005.

Hyman, J. D., Gable, C. W., Painter, S. L., and Makedonska, N. (2014). "Conforming Delaunay triangulation of stochastically generated three dimensional discrete fracture networks: A feature rejection algorithm for meshing strategy." *SIAM Journal on Scientific Computing*, Vol. 36, No. 4, A1871-A1894, DOI. 10.1137/130942541.

Itasca (2004). "3DEC user's guide Version 4.0." Itasca Consulting Group Inc.

Jeong, W. C., Kim, J. Y, and Song, J. W. (2004). "A numerical study on the influence of fault zone heterogeneity in fractured rock media." *KSCE Journal of Civil Engineering*, Vol. 8, No. 5, pp. 575-588, DOI: 10.1007/BF02899582.

Jin, F., Zhang, C. H., Wang, G. and Wang, G. L. (2003). "Creep modeling in excavation analysis of a high rock slope." *Journal of Geotechnical and Geoenvironmental Engineering*, Vol. 129, No. 9, pp. 849-857, DOI: 10.1061/(ASCE)1090-0241(2003)129:9(849).

Jing, L. (2003). "A review of techniques, advances and outstanding issues in numerical modelling for rock mechanics and rock engineering." *International Journal of Rock Mechanics and Mining Sciences*, Vol. 40, No. 3, pp. 283-353, DOI: 10.1016/S1365-1609(03)00013-3.

Jing, L., Ma, Y., and Fang, Z. (2001). "Modeling of fluid flow and solid deformation for fractured rocks with Discontinuous Deformation Analysis (DDA) method." *International Journal of Rock Mechanics and Mining Sciences*, Vol. 38, No. 3, pp. 343-355, DOI: 10.1016/S1365-1609(01)00005-3.

Jing, L., Min, K. B., Baghbanan, A., and Zhao, Z. (2013). "Understanding coupled stress, flow and transport processes in fractured rocks." *Geosystem Engineering*, Vol. 16, No. 1, pp. 2-25, DOI: 10.1080/12269328.2013.780709.

Jing, L., Tsang, C. F., and Stephansson, O. (1995). "DECOVALEX—an international co-operative research project on mathematical models of coupled THM processes for safety analysis of radioactive waste repositories." *International Journal of Rock Mechanics and Mining Sciences,* Vol. 32, pp. 389-398, DOI: 10.1016/0148-9062(95)00031-B.

Karimi-Fard, M. and Durlofsky, L. (2016). "A general gridding, discretization, and coarsening methodology for modeling flow in porous formations with discrete geological features." *Advances in Water Resources*, Vol. 96, pp. 354-372, DOI: 10.1016/j.advwatres.2016.07.019.

Koudina, N., Garcia, R. G., Thovert, J. F., and Adler, P. (1998). "Permeability of three-dimensional fracture networks." *Physical Review E*, Vol. 57, No. 4, pp. 4466-4479, DOI: 1063-651X/98/57(4)/4466(14).

Latham, J. P., Xiang, J., Belayneh, M., Nick, H. M., Tsang, C. F., and Blunt, M. J. (2013). "Modelling stress-dependent permeability in fractured rock including effects of propagating and bending fractures." *International Journal of Rock Mechanics and Mining Sciences*, Vol. 57, pp. 100-112, DOI: 10.1016/j.ijrmms.2012.08.002.

Lee, J., Choi, S., and Cho, W. (1999). "A comparative study of dual-porosity model and discrete fracture network model." *KSCE Jounnal of Civil Engineering*, Vol 3, No. 2, pp. 171-180, DOI: 10.1007/BF02829057.

Lei, Q., Latham, J. P., and Tsang, C. F. (2017). "The use of discrete fracture networks for modelling coupled geomechanical and hydrological behaviour of fractured rocks." *Computers and Geotechnics*, Vol. 85, pp. 151-176, DOI: 10.1016/j.compgeo.2016.12.024.

Lei, Q., Latham, J. P., Xiang, J., and Tsang, C. F. (2015). "Polyaxial stress-induced variable aperture model for persistent 3D fracture networks." *Geomechanics for Energy and the Environment*, Vol. 1, pp. 34-47, DOI: 10.1016/j.gete.2015.03.003.

Lei, Q., Wang, X., Xiang, J., and Latham, J. P. (2017). "Polyaxial stress-dependent permeability of a three-dimensional fractured rock layer."

Hydrogeology J, pp. 1-12, DOI: 10.1007/s10040-017-1624-y.

Mäkel, G. (2007). "The modelling of fractured reservoirs: Constraints and potential for fracture network geometry and hydraulics analysis." *Geological Society*, London, Special Publications, Vol. 292, No. 1, pp. 375-403, DOI: 10.1144/SP292.21.

Mi, L., Jiang, H., Mou, S., Li, J., Pei, Y., and Liu, C. (2016). "Numerical simulation study of shale gas reservoir with stress-dependent fracture conductivity using multiscale discrete fracture network model." *Particulate Science and Technology,* Vol. 36, pp. 1-10, DOI: 10.1080/02726351.2016.1241844.

Min, K. B., Rutqvist, J., Tsang, C. F., and Jing, L. (2004). "Stress-dependent permeability of fractured rock masses: A numerical study." *International Journal of Rock Mechanics and Mining Sciences*, Vol. 41, No. 7, pp. 1191-1210, DOI: 10.1016/j.ijrmms.2004.05.005.

Minkoff, S. E., Stone, C. M., Bryant, S., Peszynska, M., and Wheeler, M. F. (2003). "Coupled fluid flow and geomechanical deformation modeling." *Journal of Petroleum Science and Engineering*, Vol. 38, No. 1, pp. 37-56, DOI: 10.1016/S0920-4105(03)00021-4.

Mohajerani, S., Baghbanan, A., Wang, G., and Forouhandeh, S. (2017). "An efficient algorithm for simulating grout propagation in 2D discrete fracture networks." *International Journal of Rock Mechanics and Mining Sciences*, Vol. 98, pp. 67-77, DOI: 10.1016/j.ijrmms.2017.07.015.

Mohajerani, S., Huang, D., Wang, G., Jalali, S. M. E., and Torabi, S. R. (2018). "An efficient algorithm for generation of conforming mesh for three-dimensional discrete fracture networks." *Engineering Computations*, in press.

Monteagudo, J. and Firoozabadi, A. (2004). "Control volume method for numerical simulation of two phase immiscible flow in two-and three-dimensional discrete fractured media." *Water Resources Research*, Vol. 40, No. 7, DOI: 10.1029/2003WR002996.

Mustapha, H., Dimitrakopoulos, R., Graf, T., and Firoozabadi, A. (2011). "An efficient method for discretizing 3D fractured media for subsurface flow and transport simulations." *International Journal for Numerical Methods in Fluids*, Vol. 67, No. 5, pp. 651-670, DOI: 10.1002/fld.2383.

Noorishad, J., Ayatollahi, M., and Witherspoon, P. (1982). "A finite-element method for coupled stress and fluid flow analysis in fractured rock masses." *International Journal of Rock Mechanics and Mining Sciences Geomechanics Abstracts,* Vol. 19, No. 4, pp. 185-193, DOI: 10.1016/0148-9062(82)90888-9.

Noorishad, J., Tsang, C. F., and Witherspoon, P. (1992). "Theoretical and field studies of coupled hydromechanical behaviour of fractured rocks—1. Development and verification of a numerical simulator." *International Journal of Rock Mechanics and Mining Sciences Geomechanics Abstracts*, Vol. 29, pp. 401-409, DOI: 10.1016/0148-9062(92)90515-2.

Oda, M. (1986). "An equivalent continuum model for coupled stress and fluid flow analysis in jointed rock masses." *Water Resources Research*, Vol. 22, No. 13, pp. 1845-1856, DOI: 10.1029/WR022i013p01845.

Öhman, J., Niemi, A., and Tsang, C. F. (2005). "Probabilistic estimation of fracture transmissivity from wellbore hydraulic data accounting for depth-dependent anisotropic rock stress." *International Journal of Rock Mechanics and Mining Sciences*, Vol. 42, No. 5, pp. 793-804, DOI: 10.1016/j.ijrmms.2005.03.016.

Priest, S. D. (2012). *Discontinuity analysis for rock engineering*. Springer, Netherlands, DOI: 10.1007/978-94-011-1498-1.

Raghavan, R. and Chin, L. (2002). "Productivity changes in reservoirs with stress-dependent permeability." *SPE Annual Technical Conference and Exhibition.* Society of Petroleum Engineers. DOI: 10.2118/88870-PA.

Rutqvist, J., Noorishadm J., Stephansson, O., and Tsang, C. F. (1992). "Theoretical and field studies of coupled hydromechanical behaviour of fractured rocks—2. Field experiment and modelling." *International Journal of Rock Mechanics and Mining Sciences*, Vol. 29, pp. 411-419, DOI: 10.1016/0148-9062(92)90515-2.

Rutqvist, J. and Stephansson, O. (2003). "The role of hydromechanical coupling in fractured rock engineering." *Hydrogeology J*, Vol. 11, No. 1, pp. 7-40, DOI: 10.1007/s10040-002-0241-5.

Somerton, W. H., Söylemezoğlu, I., and Dudley, R. (1975). "Effect of stress on permeability of coal." *International Journal of Rock Mechanics and Mining Sciences*, Vol. 12, pp. 129-145, DOI: 10.1016/0148-9062(75)91244-9.

Son, M. and Moon, H. K. (2017). "The hydraulic stability assessment of jointed rock mass by analysis of stress path due to underground excavation." *KSCE Journal of Civil Engineernig*, Vol 21, Issue 6, pp. 2450-2458, DOI: 10.1007/s12205-016-1017-0.

Vairogs, J., Hearn, C., Dareing, D. W., and Rhoades. V. (1971). "Effect of rock stress on gas production from low-permeability reservoirs." *Journal of Petroleum Technology*, Vol 23, No. 9, pp. 161-161, 167, DOI: 10.2118/3001-PA.

Vermilye, J. M. and Scholz, C. H. (1995). "Relation between vein length and aperture." *Journal of Structural Geology*, Vol. 17, No. 3, pp. 423-434, DOI: 10.1016/0191-8141(94)00058-8.

Xie, Y. and Wang, G. (2014). "A stabilized iterative scheme for coupled hydro-mechanical systems using reproducing kernel particle method." *International Journal for Numerical Methods in Engineering*, Vol. 99, pp. 819-843, DOI: 10.1002/nme.4704.

Xie, N., Yang, J., and Shao, J. (2015). "Study on the hydromechanical behavior of single fracture under normal stresses." *KSCE Journal of Civil Engineering*, Vol. 18, No. 6, pp. 1641-1649, DOI: 10.1007/s12205-014-0490-6.

Xu, C. and Dowd, P. (2010). "A new computer code for discrete fracture network modelling." *Computers & Geosciences*, Vol. 36, No. 3, pp. 292-301, DOI: 10.1016/j.cageo.2009.05.012.

Ye, J. H., Huang, D., and Wang, G. (2016). "Nonlinear dynamic simulation of offshore breakwater on sloping liquefied seabed." *Bulletin of Engineering Geology and the Environment*, Vol. 75, pp. 1215-1225, DOI: 10.1007/s10064-016-0906-2.

Ye, J. H. and Wang, G. (2016). "Numerical simulation of the seismic liquefaction mechanism in an offshore loosely deposited seabed." *Bulletin of Engineering Geology and the Environment*, Vol. 75, pp. 1183-1197, DOI: 10.1007/s10064-015-0803-0.

Zareifard, M. R. and Fahimifar, A. (2016). "A simplified solution for stresses around lined pressure tunnels considering non-radial symmetrical seepage flow." *KSCE Journal of Civil Engineering*, Vol. 20, No. 7, pp. 2640-2654, DOI: 10.1007/s12205-016-0105-5.

Zhang, J., Standifird, W., Roegiers, J. C., and Zhang, Y. (2007). "Stress-dependent fluid flow and permeability in fractured media: From lab experiments to engineering applications." *Rock Mechanics and Rock Engineering*, Vol. 40, No. 1, pp. 3-21, DOI: 10.1007/s00603-006-0103-x

Zhao, Z., Rutqvist, J., and Leung, C. (2015). "Impact of stress on solute transport in a fracture network: A comparison study." *Journal of Rock Mechanics and Geotechnical Engineering*, Vol. 5, No. 2, pp. 110-123, DOI: 10.1016/j.jrmge.2013.01.002.

Zimmerman, R. and Main, I. (2004). "Hydromechanical behavior of fractured rocks." *International Geophysics,* Vol. 89, pp. 363-422, DOI: 10.1016/S0074-6142(03)80023-2.